Science of the Total Environment 615 (2018) 462–468

Contents lists available at ScienceDirect

Science of the Total Environment

journal homepage: www.elsevier.com/locate/scitotenv

Degradation of nonylphenol polyethoxylates by functionalized Fe_3O_4 nanoparticle-immobilized *Sphingomonas* sp. Y2

Naling Bai [a,b], Sheng Wang [a], Pengfei Sun [c], Rexiding Abuduaini [a], Xufen Zhu [d], Yuhua Zhao [a,*]

[a] Institute of Microbiology, College of Life Sciences, Zhejiang University, Hangzhou 310058, China
[b] Eco-environmental Protection Research Institute, Shanghai Academy of Agricultural Science, Shanghai 201106, China
[c] State Key Laboratory of Soil and Sustainable Agriculture, Institute of Soil Science, Chinese Academy of Sciences, Nanjing 210008, China
[d] Institute of Genetics, College of Life Sciences, Zhejiang University, Hangzhou 310058, China

HIGHLIGHTS

- NPEOs-degrading *Sphingomonas* sp. Y2 was immobilized on PD-IONPs yielding Y2-PD-IONPs.
- Y2-PD-IONPs have the advantages of good degradation efficiency, stability, reusability, and easy separation.
- Y2-PD-IONPs retained over 70.0% degradation activity after 6 cycles of utilization.
- Y2-PD-IONPs can be used for biodegradation of NPEOs in simulated-textile wastewater.

GRAPHICAL ABSTRACT

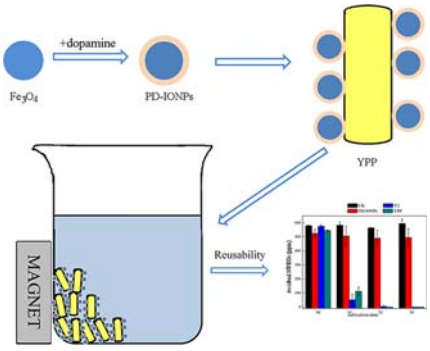

ARTICLE INFO

Article history:
Received 18 July 2017
Received in revised form 25 September 2017
Accepted 27 September 2017
Available online xxxx

Editor: Jay Gan

Keywords:
Nonylphenol polyethoxylate
Magnetic nanoparticles
Polydopamine
Immobilization
Biodegradation

ABSTRACT

In this study, the efficiency of the nonylphenol polyethoxylates (NPEOs)-degrading bacterium *Sphingomonas* sp. strain Y2 was evaluated, which was immobilized by a novel system composed of polydopamine (PD)-coated Fe_3O_4 iron nanoparticles (IONPs). The PD-IONPs, with a distinct core-shell structure, relatively uniform size, and high saturation magnetization, were prepared for Y2 immobilization. The performance of Y2 was unaffected by this novel immobilization method, exhibiting 79.5% and 99.9% of NPEOs (500 ppm) degradation efficiency at day 1 and 2, respectively. Furthermore, separation and recycling were more readily achieved for immobilized cells as compared to free cells. Immobilized cells retained over 70% of the original degradation activity after 6 cycles of utilization. These results suggest that Y2-PD-IONPs can be potentially used for NPEOs-contaminated wastewater bioremediation.
Capsule: Immobilization of *Sphingomonas* sp. Y2 by functionalized PD-IONPs with easy separation, recycling utilization and high efficiency.

1. Introduction

Nonylphenol polyethoxylates (NPEOs) are a family of non-ionic surfactants that are widely used in industrial, agricultural, and household applications (Lin et al., 2016). They can easily enter aquatic environments and cause extensive pollution (Sun et al., 2014). For example,

* Corresponding author.
E-mail address: yhzhao225@zju.edu.cn (Y. Zhao).

https://doi.org/10.1016/j.scitotenv.2017.09.290
0048-9697/

the concentrations of NPEOs in some real samples such as white silk fabric, flax/cotton blended fabric, and wool/nylon/cotton blended fabric were reported to be 2763, 1837, and 783 mg/kg, respectively (Zhang et al., 2007). The contents of nonylphenol (NP) and NPEOs detected in an oil harbor were 64.8 and 395 ng/L and those detected in Haichang Xincheng were 732.2 and 702.5 ng/L, respectively, which were significantly higher than the levels reported at other sampling sites (Wang et al., 2011). Furthermore, Naylor et al. (1992) found that a majority of sediment samples contained detectable amounts of NP and NPE1O, ranging up to 3000 ppb and 170 ppb, respectively. Berryman et al. (2004) analyzed 11 kinds of drinking water treatment plants located downstream of textile plants or pulp and paper mills, and found that approximately 20% of the samples exceeded the Canadian 1 μg/L NP water quality guideline; some results even exceeded Quebec's 6 μg/L guideline for the limit of NP levels. In addition, this type of surfactant is known to be toxic and interferes with endogenous hormone systems by mimicking estrogen compounds. Notably, the metabolites, including NP, short-chain NPEOs (n = 1–3), and NPEO-carboxylates in that order are more toxic than the parent molecules (Lin et al., 2016; Staples et al., 2004). For instance, the cell survival rate decreased by about 25%, 55%, and 88%, respectively, after treatment with 100, 300, and 500 μM NP10EO for 24 h (Toyooka et al., 2012). NPEOs with ethylene oxide (EO) units in the range of 0–15 would more readily induce the phosphorylation of histone H2AX, which could lead to double-stranded DNA breaks (Toyooka et al., 2012). Furthermore, NP and NP10EO were both found to be toxic to *Moina macrocopa*, with the toxicity of NP being stronger: the 24-h LC50 values of NP and NP10EO to *M. macrocopa* were 0.154 mg/L and 3.37 mg/L, and the 48-h LC50 values were 0.065 mg/L and 2.11 mg/L, respectively. The 24-h and 48-h LC50 values of the mixed exposure were 0.646 TU and 0.291 TU, respectively, indicating that they had a strong synergistic effect (Hu, 2012). Given the high level of environmental pollution and toxicity effects caused by nonylphenic compounds, efficient transformation and mineralization are urgent needed.

Bioremediation is a low-cost, environmentally safe approach to remove NPEOs and their metabolites from the environment (Zhuang et al., 2015). However, the application of NPEOs-degrading microorganisms in the environment depends on their ability to survive microfaunal predators and abiotic stresses (Jousset, 2012). To this end, different methods of bacterial immobilization have been developed such as entrapment in alginate beads, adsorption of bacteria on support materials, and cross linkage with carriers. However, these approaches have limitations including substrate diffusion, poor cellular recovery, or adsorption (Deng et al., 2016a; Lu, 2013).

Nanotechnology provides many advantages for environmental remediation such as effective feeder loading, large surface area, and mechanical strength (Lu et al., 2012; Xu et al., 2012). For example, carbon nanomaterials are promising candidates for enzyme immobilization since they are chemically inert, biocompatible, and electrically conductive (Mundra et al., 2014). Significantly, iron oxide-based magnetic nanoparticles have potential biomedical, analytical, environmental, and industrial applications due to their ease of separation and delivery, large surface area, controllable synthesis and surface modification, high biocompatibility, recyclability, and low toxicity (Lu et al., 2007a; Xu et al., 2012). Gu et al. (2003) reported that vancomycin-conjugated FePt nanoparticles facilitated the capture and detection of low levels of pathogen rapidly. Coating of a magnesium–aluminum double hydroxides layer on magnetic nanoparticles (Fe_3O_4@MgAlLDHs nanoparticles) combined with supramolecular solvents as the magnetic supramolecular fluids were successfully applied to the extraction and determination of four phenolic compounds (Yang et al., 2017). However, naked metallic nanoparticles are highly reactive and readily oxidized in air, which results in the loss of magnetism and dispersibility (Lu et al., 2007a). In order to improve immobilization efficiency, naked nanoparticles must be chemically stabilized against degradation during and after synthesis (Martín et al., 2014; Pan et al., 2012).

Nanoparticles can be modified by stabilizers, electrostatic surfactants, and steric polymers (Xu et al., 2012). In general, polymers can be chemically anchored or physically adsorbed onto magnetic nanoparticles to form layers to stabilize repulsive forces (Lu et al., 2007a). Dopamine (DA) is a catecholamine neurotransmitter associated with many physiological processes, and has recently been proposed as a novel organic coating material (Hou et al., 2015a). It can self-polymerize in aerated basic solutions, forming an adherent polydopamine (PD) film over organic or inorganic surfaces. Functional groups on PD film can be used to anchor other components. Furthermore, it was recently reported that nitration of the catechol of PD enhanced the stability of PD-based anchors on IONPs, providing more options for their surface modification in physiological applications (Amstad et al., 2009).

We immobilized the bacterium *Sphingomonas* sp. Y2 and investigated its performance in terms of NPEOs degradation. The findings can offer primary guidelines for the removal of NPEOs in wastewater.

2. Materials and methods

2.1. Materials

Commercially available NPEOs with an average ethoxylate chain length of 9 (CAS No. 9016-45-9, ~10%) were purchased from Aladdin Industrial Corporation (Shanghai, China). Ferric chloride hexahydrate, ferrous chloride tetrahydrate, and sodium hydroxide were obtained from Sinopharm Chemical Reagent Co. (Beijing, China). DA hydrochloride and Tris base were from Sigma-Aldrich (St. Louis, MO, USA) and Sangon Co. (Shanghai, China), respectively. Other chemicals were all of analytical grade.

Strain Y2, isolated from activated sludge from Shaoxing, Zhejiang Province, China and identified as *Sphingomonas* in our previous study (Bai et al., 2016), was cultured in 100 mL mineral salt medium (MSM) with 500 ppm NPEOs as the sole carbon source and 100 ppm ampicillin in a horizontal shaker at 200 rpm and 30 °C for 2 days.

2.2. Preparation of IONPs and PD-IONPs

Magnetic Fe_3O_4 Nanoparticles were prepared by modified chemical co-precipitation (Chen et al., 2011), as follows: 9.9 g $FeCl_2$ and 27.0 g $FeCl_3$ were dissolved in 100 mL sterilized water under vigorous magnetic stirring; the pH was adjusted to 10.0 by dropwise addition of 5 M NH_4OH solution with constant stirring at 80 °C for 1 h. The solution was centrifuged at 3600 × *g* for 10 min, and the precipitate was washed with ethyl alcohol and distilled water for neutralization and oven-dried (60 °C) to a constant weight, yielding Fe_3O_4 iron oxide nanoparticles (IONPs).

IONPs were suspended in 10 mM Tris-HCl buffer (pH 8.5) to a final concentration of 1 mg/mL. After ultrasonication for 30 min, large particles were discarded and DA was added to the IONPs suspension at 1 mg/mL at room temperature; self-polymerization can be achieved in aerated alkane solutions to form an adherent PD film. A 5-mL aliquot of the suspension was removed and separated with a strong magnet; excess DA in the aqueous phase was discarded. PD-coated IONPs (PD-IONPs) were rinsed three times with sterilized water and stored at 4 °C.

2.3. Immobilization of Sphingomonas sp. Y2

PD-IONPs (1 mg/mL) were dispersed in bacterial solution (2 mg/mL) at a volume ratio of 1:10, and immobilization was carried out at 4 °C on a shaker at 150 rpm for 2 h. Immobilized Y2 was collected by magnetic separation and washed three times with phosphate-buffered saline (PBS) to remove unreacted Y2. The resultant Y2-PD-IONPs (YPP) was stored at 4 °C. Immobilization efficiency was measured as the change of optical density at 600 nm (OD_{600}).

2.4. Characterization of IONPs, PD-IONPs, and YPP

Particle morphology was analyzed by transmission electron microscopy (JEM-1200EX; JEOL, Tokyo, Japan) followed by energy dispersion spectroscopy (EDS) (Siron; FEI, Eindhoven, the Netherlands). Magnetization measurements were obtained using a multi-functional vibrating sample magnetometer (J3426; Cryogenic, London, UK). The Fourier transform infrared (FTIR) spectra of unmodified IONPs and PD-IONPs were recorded in the region of 2000–500 cm^{-1} on a Perkin-Elmer spectrophotometer (AVA TAR370; Thermo Fisher Scientific, Waltham, MA, USA) using the KBr pellet technique. After vacuum freeze drying, the thermal stability of samples was determined using a thermogravimetric (TG) analyzer (Q50; TA Instruments, New Castle, DE, USA), and the program was set to heat from 50 °C to 750 °C at a rate of 10 °C/min under a nitrogen atmosphere.

2.5. Determination of immobilization efficiency

The thickness of PD films plays an important role in immobilization efficiency, which is dependent on self-polymerization reaction time (Lu, 2013). The detailed reaction conditions are the same as those described above in Section 2.2. Immobilization efficiency (R) was evaluated by the amount of Y2 bound to the materials supporting the unit mass in order to determine the optimum time required for PD attachment onto IONPs according to the formula: $R = (OD_0 - OD_t) / OD_0 \times 100\%$, where OD_0 is the initial biomass of Y2 (2 mg/mL), which was 0.54; and t is the specific reaction time of PD attaching to IONPs, which was 0.25, 0.5, 1, 2, 3, and 4 h. Meanwhile, the concentration of immobilized Y2 cells was measured by calculating the difference in the concentration before and after Y2 immobilization: $\Delta OD = OD_0 - OD_t$. Each sample was measured in duplicate.

2.6. NPEOs biodegradation by YPP and reusability

The degradation efficiency of YPP was evaluated by measuring NPEOs removal. Free and immobilized bacteria were cultured as resting cells in 10-mL of MSM without adding trace elements, and the biomass was estimated as $OD_{600} = 0.25$. The initial NPEOs concentration was set as 500 ppm, and the residual substrate was examined every day over the 3 days of cultivation. Samples only supplemented with NPEOs were set as blank control; samples with substrate NPEOs and modified nanoparticles PD-IONPs were considered as background control. A 1-mL aliquot of the sample was removed by centrifugation and magnetic separation of Y2 and YPP, respectively. Then a 500-μL sample was withdrawn and extracted with isometric methanol for 30 min before filtration through a 0.22-μm polyvinylidene difluoride filter membrane. High-performance liquid chromatography (HPLC) was carried out as previously described (Bai et al., 2016), except that the mobile phase was methanol/water (v/v) = 90/10. The degradation efficiency was calculated as: $(C_0 - C_t) / C_0 \times 100\%$, where C_0 and C_t are NPEOs concentrations at initial and specific biodegradation periods, respectively. All samples were prepared in triplicate.

The reusability of immobilized cells was determined by measuring the amount of NPEOs after degradation by recovered YPP. The time frame for each round of biodegradation monitoring was 3 days. At each sampling time point, YPP was magnetically separated and Y2 was centrifuged and rinsed three times with PBS buffer. Free cells and samples without incubation served as control groups.

A solution of intermediates was obtained by centrifugation of the NPEOs biodegradation medium; then PD-IONPs and YPP absorption were determined. An appropriate amount (0.5 mg/mL) of PD-IONPs or YPP was added to the 10-mL sample. The nanoparticles were magnetically separated and samples were sacrificed and extracted twice with equal volumes of chloroform. After evaporating the solvent, intermediates were redissolved in 2.5 mL methanol and analyzed by HPLC as previously described (Bai et al., 2016).

2.7. Application of YPP to simulated textile-dyeing wastewater

The textile industry is an important part of manufacturing productivity, employment, and economic trade in many countries (Karci, 2014). NPEOs and their analogs are widely used in industry (Ciofi et al., 2016). We investigated the applicability of immobilized Y2, YPP, to NPEOs biodegradation using simulated textile-dyeing wastewater (STW) composed of (ppm): glucose (600), Reactive Black (12.3), $(NH_4)_2SO_4$ (140), KH_2PO_4 (26), $NaHCO_3$ (120), Na_2SO_4 (70), and NPEOs (120) (pH = 9.0). After sterilization at 115 °C for 30 min, NPEOs were added to 10 mL STW followed by the addition of 2 mL YPP; an equal mass of Y2 was used as a positive control (OD_{600} = 0.25) and STW without incubation served as a blank control. The degradation efficiency was analyzed on days 3, 6, and 12. Extraction and detection were carried out as described above. YPP was magnetically separated while Y2 was concentrated by centrifugation at 10,000 × *g* for 5 min.

3. Results and discussion

3.1. Characterization of IONPs, PD-IONPs, and YPP

The main experimental challenge in Fe_3O_4 synthesis by co-precipitation is controlling particle size distribution and dispersibility (Lu et al., 2007a). The characteristics of materials are presented in Fig. 1. In our study, IONPs were prepared by chemical co-precipitation in alkali media. The particles were spherical, with an average size

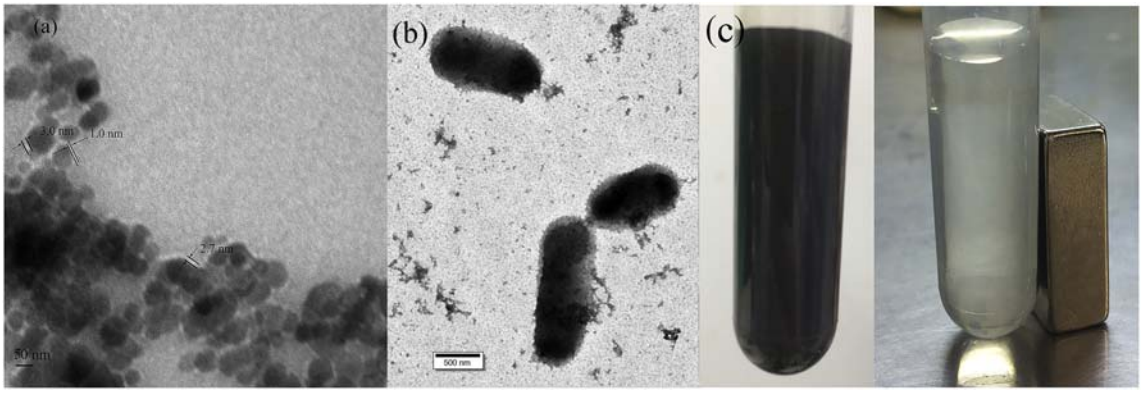

Fig. 1. Images of IONPs, PD-IONPs, and YPP biocomposite. (a) Transmission electron micrographs of PD-IONPs. (b) Micrographs of YPP composite. (c) YPP concentrated and collected using an external magnet.

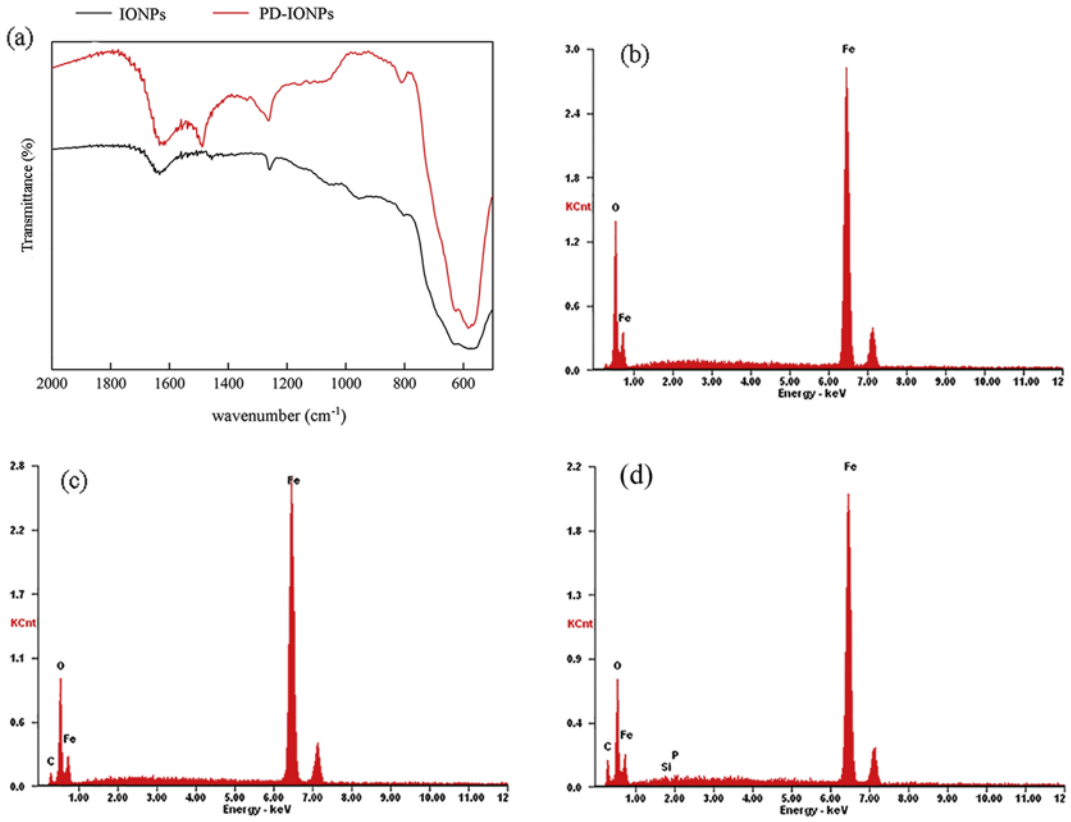

Fig. 2. (a) FTIR analysis of IONPs (black) and PD-IONPs (red). (b–d) EDS analysis of IONPs (b), PD-IONPs (c), and YPP (d). (For interpretation of the references to colour in this figure legend, the reader is referred to the web version of this article.)

smaller than 20 nm. Particles with a diameter < 30 nm exhibit superparamagnetic properties (Lee et al., 1996), although they tend aggregate due to intrinsically high surface energy (Martín et al., 2014). IONPs were coated with thin PD film through spontaneous oxygen-mediated self-polymerization in an aqueous solution of pH 8.5, yielding an IONPs core trapped by a thin PD layer of approximately 2.23 ± 1.08 nm (Fig. 1a). The Y2 surface was coated with PD-IONPs (Fig. 1b). The YPP biocomposite was easily separated and collected by means of an externally applied magnetic field, due to the superparamagnetic properties of IONPs. YPP aggregated at the site of contact between the tube and cell suspension, and the separation required no further optimization (Fig. 1c).

FTIR spectra of IONPs and PD-IONPs are shown in Fig. 2a. The peaks at around 630 and 576 cm^{-1} were attributed to the Fe—O bond of Fe_3O_4 magnetic nanoparticles (Do Kim et al., 2007; Han et al., 2015; Sun et al., 2015), indicating the presence of Fe_3O_4 in the two samples. The peak at 811 cm^{-1} in the spectrum of PD-IONPs reflected the vibration of the N—H bond (Do Kim et al., 2007), whereas the band at 1250 cm^{-1} corresponded to phenolic hydroxyl group stretching vibrations of the PD layer (Deng et al., 2016b). Vibrational signals at 1630 and 1490 cm^{-1} were caused by C—C in aromatic rings. These peaks revealed the interaction of PD with Fe_3O_4. The absorption of IONPs at 600–1800 cm^{-1} was not as smooth as previously reported (Han et al., 2015), which may be due to the simplified procedure of nanoparticles preparation without inert atmosphere protection (Lu et al., 2007a).

The main elements of IONPs, PD-IONPs, and YPP were investigated by EDS (Fig. 2b–d). All three contained varying degrees of iron, which peaked at 6.5 keV: Fe and O comprised over 95% (wt%) of IONPs, with

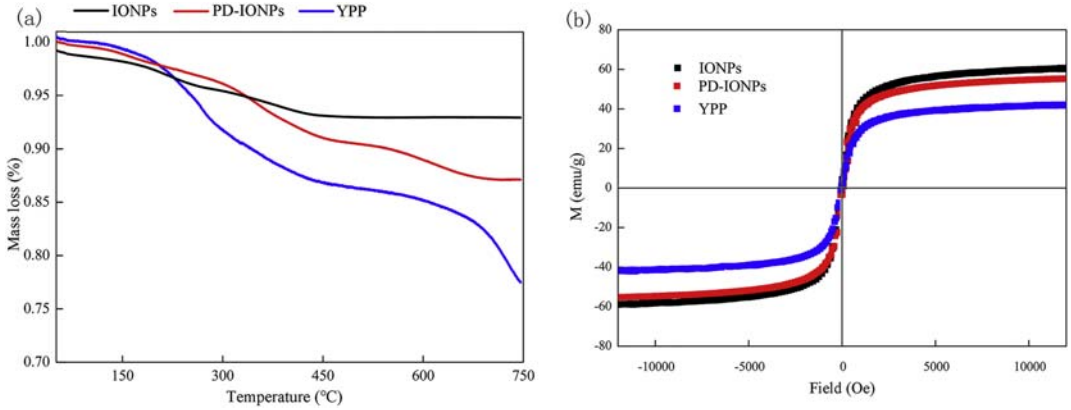

Fig. 3. (a) TG curves of IONPs, PD-IONPs, and YPP. (b) Hysteresis loop of magnetic nanoparticles before and after binding to Y2 cells.

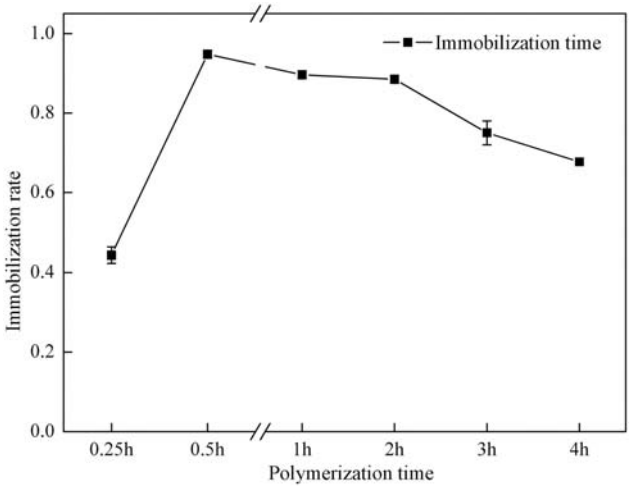

Fig. 4. Immobilization efficiency of YPP with different polymerization times of PD.

an Fe/O mass ratio of 2.77 corresponding to pure Fe_3O_4 (2.62), whereas carbon atoms accounted for 10.06% of PD-IONPs, and were attributed to PD films. YPP, contained C, O, Si, P, and Fe atoms, and Fe content was only 58.16%, suggesting incorporation of Y2 .

The TG curve of bare IONPs, PD-IONPs, and YPP are shown in Fig. 3a. Unmodified IONPs showed a slight loss of 2.61% below 200 °C and an additional loss of 4.42% in the range of 200–750 °C, providing evidence for their thermal stability. A similar trend was observed for PD-IONPs with a loss of 10.83% as the temperature reached 200 °C to 750 °C, suggesting PD decomposition. For YPP, when the temperature was below 200 °C, the rate of mass loss was slightly higher than for the other two samples, which may be attributed to the bacterial cells; that is, after Y2 immobilization, an additional loss of 20.61% was observed as compared to PD-IONPs at 750 °C.

The most important aspect of IONPs decoration is the retention of sufficient magnetic properties. This was examined for IONPs, PD-IONPs, and YPP at room temperature using a multi-functional vibrating magnetometer (Fig. 3b). The magnetic saturation (MS) of IONPs, PD-IONPs, and YPP were 62.40, 56.80, and 44.27 emu/g, respectively. In contrast, the values for magnetic nanoparticles synthesized by co-precipitation is in the range of 30–50 emu/g, which is lower than the bulk value of 90 emu/g (Lu et al., 2007a). The MS of oleate-modified IONPs and magnetically coated *Rhodococcus* sp. LSSE8-1 was 50.8 and 14.3 emu/g, respectively (Li et al., 2009). Furthermore, the MS of Fe_3O_4 nanoparticles and porous magnetic polymer microspheres fabricated by an inverse replication method was 10.81 and 5.15 emu/g, respectively (Han et al., 2015). The relatively high MS value of YPP indicated its effective separation. On the other hand, the lower MS of PD-IONPs and YPP compared to IONPs was due to the added mass of PD and Y2 on the surface (Hou et al., 2015c). Organic ligands used to stabilize magnetic nanoparticles may influence their magnetic properties (Lu et al., 2007a). The fact that the particles were easily collected within several minutes by applying a magnet suggests that the bacterium did not inhabit the rapid magnetic response of the support material.

3.2. Immobilization efficiency

The amino and thiol groups in many macromolecules can form Schiff bases and/or Michaelis addition adducts with the catechols in PD, and active groups on the surface of PD films can serve as anchors for further chemical modification or immobilization of biologically active molecules (Liu et al., 2014). Robust interfacial binding forces between the coating and substrate through covalent bonds or other intermolecular interactions allow PD to be easily adapted to a variety of materials without requiring surface pretreatment. Y2 cells were immobilized on PD-IONPs via covalent bonding. The effect of self-polymerization time on percentage immobilization was evaluated (Fig. 4). The immobilization efficiency increased dramatically from 44.3% to 94.8% and then decreased to 67.7% along with polymerization time of PD. We therefore selected 0.5 h as the optimal reaction time, i.e., the point at which PD has completely covered the surface of bare nanoparticles and had the most covalent binding sites. Too much PD led to a decrease in the specific surface area of PD-IONPs carrier, which would affect cell immobilization and the whole degradation efficiency (data not shown). Initially, the coating of PD would dramatically increase the binding capacity to cells. However, after reaching the critical value, the binding capacity of PD-IONPs would decrease (Chen et al., 2011). Longer reaction times would not further increase the number of binding sites or immobilization efficiency.

3.3. NPEOs degradation by YPP

A simple reversed-phase HPLC method was used to evaluate the removal efficiency of NPEOs, and the chromatogram of NPEOs was shown in Fig. 5a. All oligomers of NPEOs were co-eluted as a single peak with the relative retention time of 5.829 min (Fig. 5a), indicating that this analysis method was suitable for monitoring the change curves of NPEOs concentration(Lu et al., 2007b). NPEOs degradation by free and immobilized Y2 was compared (Fig. 5b). There was little adsorption of NPEOs by PD-IONPs, in contrast to a previous report that

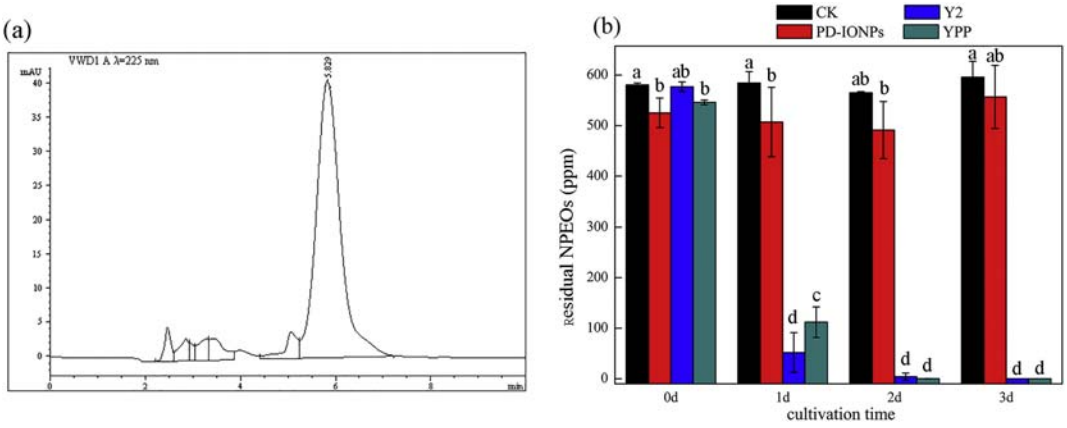

Fig. 5. (a) Typical reversed-phase HPLC chromatogram for NPEOs at the beginning of the experiment. (b) Degradation of NPEOs in MSM by Y2 or YPP. The initial NPEOs concentration was 500 ppm, which served as the sole carbon source and energy source. Different lower case letters above the columns represent statistically significant differences ($p < 0.05$).

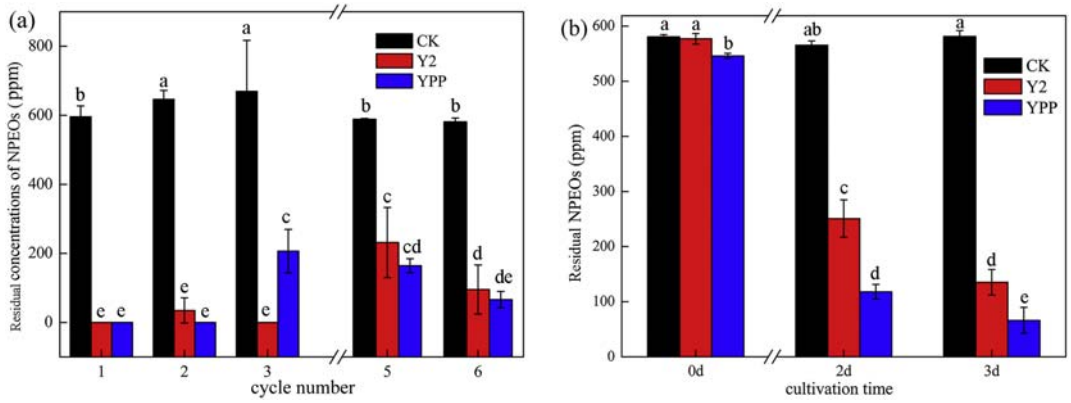

Fig. 6. (a) Reusability of YPP. (b) Degradation efficiency of YPP in the sixth cycle of utilization. The initial NPEOs concentration was 500 ppm, which served as the sole carbon source and energy source. Different lower case letters above the columns represent statistically significant differences ($p < 0.05$).

polyethylenimine-PD/graphene oxide composite nanosheets efficiently adsorbed heavy metals (Dong et al., 2015). This is likely due to the innate non-ionic character of NPEOs. *Bacillus clausii* BS1 decorated with Fe_3O_4 had higher denitrogenation activity than the free cells, which was attributed to the reversible adsorption/desorption between Fe_3O_4 and carbazole (Zakaria et al., 2015). The degradation efficiencies of free and coated Y2 were highly similar throughout the culture period: 91.00% and 79.47% of the NPEOs were removed within day 1, respectively. The pollutant was almost depleted at later time points in both samples with the same efficiency ($p > 0.05$), suggesting that the coated nanoparticles probably did not negatively impact the mass transfer and biodegradation of NPEOs. Approximately 0.42 ± 0.01 ppm nanoparticles remaining in the residue after magnetic isolation, indicating the easy separation and low toxicity of IONPs.

Similar observations have been reported by previous studies (Li et al., 2013; Zakaria et al., 2015); that is, the coating layer did not change the characteristics of the cell surface owing to the biocompatibility of IONPs. Thus, PD can be used as an anchor for immobilizing functional molecules onto nanoparticles and does not affect magnetic separation (Xu et al., 2004). Short-chain NPEOs and short-chain NPECs, the main breakdown products of NPEOs, were determined by GC–MS as reported previously (Bai et al., 2016). However, neither PD-IONPs nor YPP adsorbed the intermediates (data not shown), which might be related to the electronegativity and valence of the target substance.

3.4. Reusability of YPP

Recycling cells can save cultivation time and reduce nutrient requirements as well as cell wastes. To determine the potential of YPP for use in industrial applications, it is important to assess its reusability. The NPEOs degradation efficiencies of Y2 and YPP were investigated in continuous cycles. The NPEOs-degrading capacity of YPP was over 70% after six rounds of utilization (Fig. 6a); in fact, during the sixth cycle, YPP removed 80% of NPEOs in 2 days, which was higher than the amount removed by Y2 (67%). The overall removal rate was also higher for YPP than for Y2 (89% vs. 77%) (Fig. 6b). The relatively high degradation efficiency of YPP was likely due to the hardness of the supporting material (Hou et al., 2015b) or higher permeability of the cell membrane (Ansari et al., 2009). Thus, PD-IONPs not only provide an effective and convenient means of separation, but also preserve the catalytic activity of cells.

3.5. Biodegradation of NPEOs in STW with YPP

Bioremediation in situ using microorganisms with high degradation efficiency is a promising approach for disposing of unwanted chemicals. The availability of specified consortia is the most important determinant of successful bioaugmentation (Mrozik and Piotrowska-Seget, 2010). Most of the previous studies on bioaugmentation with immobilized degrading consortia have been conducted using traditional methods. We therefore, explored the ability of YPP in STW to degrade NPEOs (Fig. 7). Degradation by YPP declined on days 3 and 6 relative to Y2, but the difference was not statistically significant ($p > 0.05$). At day 6, YPP and Y2 respectively removed 45.1% and 57.8% NPEOs. By the end of day 12, NPEOs was completely removed by both Y2 and YPP.

Enzyme immobilization by nanoparticles has been widely reported, but associated with its own challenges. For instance, direct PD-functionalized immobilization without a coupling reagent would likely decrease enzymatic activity by constraining the three-dimensional structure and inactivating critical residues near the active site (Gao et al., 2014; Hou et al., 2015c). Furthermore, proteins in aqueous solution tend to be inactivated by inevitable mechanical forces. These problems can be avoided by effectively immobilizing cells. Cells can be immobilized for magnetic separation and environmental remediation (Sun et al., 2015; Xu et al., 2012; Zakaria et al., 2015). For example, nanoparticles have also been used as nanosorbents to remove pollutants such as organic dyes and heavy metals (Dong et al., 2015; Xu et al., 2012). However, the electrostatic interactions in adsorption require that the target material be positively or negatively charged, which is incompatible with the nonionic NPEOs. In this study, we analyzed YPP, the mini-reactors, to degrade NPEOs in STW. The PD-IONPs not only simplified the separation operation but also increased the cell viability. The overall results indicated that YPP can be an effective candidate for bioremediation.

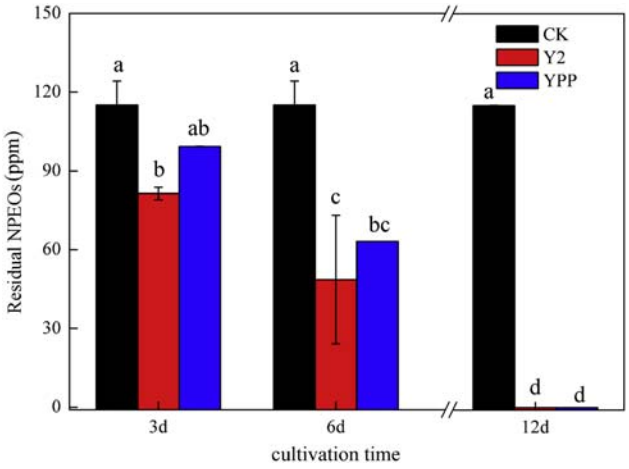

Fig. 7. Biodegradation of NPEOs in STW by YPP and Y2. The initial NPEOs concentration was 120 ppm in STW. Different lower case letters above the columns represent statistically significant differences ($p < 0.05$).

4. Conclusion

Sphingomonas sp. Y2 was decorated with PD-IONPs to facilitate cell separation following NPEOs degradation. Composite PD-IONPs exhibited superparamagnetism, monodispersity, biocompatibility, and easy separation; this series of substances was also found to show little adsorption of NPEOs and the intermediates. The coated cells, YPP, could efficiently degrade 99.9% and 100.0% of the NPEOs in MSM and STW within 2 and 12 days, respectively. Moreover, the cells retained over 70% of the original degradation activity after 6 cycles of utilization. These results demonstrated that a magnetic bio-adhesive material can be used to immobilize cells, and that YPP has practical potential to remove NPEOs from contaminated environments.

Acknowledgements

This study was supported by the National Key Basic Research Program of China (2015CB150502), the National Natural Science Foundation of China (31470191; 41671314), and the Key Research and Development Program of Zhejiang Province (2015C03011).

Conflict of interest

There are no conflicts of interest to declare. This study did not involve any human participants.

References

Amstad, E., Gillich, T., Bilecka, I., Textor, M., Reimhult, E., 2009. Ultrastable iron oxide nanoparticle colloidal suspensions using dispersants with catechol-derived anchor groups. Nano Lett. 9, 4042–4048.

Ansari, F., Grigoriev, P., Libor, S., Tothill, I.E., Ramsden, J.J.D.B.T., 2009. degradation enhancement by decorating *Rhodococcus erythropolis* IGST8 with magnetic Fe_3O_4 nanoparticles. Biotechnol. Bioeng. 102, 1505–1512.

Bai, N.L., Wang, S., Abuduaini, R., Zhu, X.F., Zhao, Y.H., 2016. Isolation and characterization of *Sphingomonas* sp. Y2 capable of high-efficiency degradation of nonylphenol polyethoxylates in wastewater. Environ. Sci. Pollut. Res. 23, 12019–12029.

Berryman, D., Houde, F., DeBlois, C., O'Shea, M., 2004. Nonylphenolic compounds in drinking and surface waters downstream of treated textile and pulp and paper effluents: a survey and preliminary assessment of their potential effects on public health and aquatic life. Chemosphere 56, 247–255.

Chen, B., Chen, Z., Lv, S.A., 2011. novel magnetic biochar efficiently sorbs organic pollutants and phosphate. Bioresour. Technol. 102, 716–723.

Ciofi, L., Ancillotti, C., Chiuminatto, U., Fibbi, D., Pasquini, B., Bruzzoniti, M.C., et al., 2016. Fully automated on-line solid phase extraction coupled to liquid chromatography–tandem mass spectrometry for the simultaneous analysis of alkylphenol polyethoxylates and their carboxylic and phenolic metabolites in wastewater samples. Anal. Bioanal. Chem. 408, 3331–3347.

Deng, F., Liao, C., Yang, C., Guo, C., Ma, L., Dang, Z.A., 2016a. new approach for pyrene bioremediation using bacteria immobilized in layer-by-layer assembled microcapsules: dynamics of soil bacterial community. RSC Adv. 6, 20654–20663.

Deng, X., Cao, S., Li, N., Wu, H., Smith, T.J., Zong, M., et al., 2016b. A magnetic biocatalyst based on mussel-inspired polydopamine and its acylation of dihydromyricetin. Chinese. J. Catal. 37, 584–595.

Do Kim, K., Min, S.S., Choa, Y.H., Kim, H.T., 2007. Formation and surface modification of Fe_3O_4 nanoparticles by co-precipitation and sol-gel method. J. Ind. Eng. Chem. 13, 1137–1141.

Dong, Z., Zhang, F., Wang, D., Liu, X., Jin, J., 2015. Polydopamine-mediated surface-functionalization of graphene oxide for heavy metal ions removal. J. Solid State Chem. 224, 88–93.

Gao, X., Ni, K., Zhao, C., Ren, Y., Wei, D., 2014. Enhancement of the activity of enzyme immobilized on polydopamine-coated iron oxide nanoparticles by rational orientation of formate dehydrogenase. J. Biotechnol. 188, 36–41.

Gu, H., Ho, P.-L., Tsang, K.W.T., Wang, L., Xu, B., 2003. Using biofunctional magnetic nanoparticles to capture vancomycin-resistant *Enterococci* and other gram-positive bacteria at ultralow concentration. J. Am. Chem. Soc. 125, 15702–15703.

Han, P., Jiang, Z., Wang, X., Wang, X., Zhang, S., Shi, J., et al., 2015. Facile preparation of porous magnetic polydopamine microspheres through an inverse replication strategy for efficient enzyme immobilization. J. Mater. Chem. B 3, 7194–7202.

Hou, C., Qi, Z.G., Zhu, H., 2015a. Preparation of core-shell magnetic polydopamine/alginate biocomposite for *Candida rugosa* lipase immobilization. Colloids Surf., B 128, 544–551.

Hou, C., Zhou, L., Zhu, H., Wang, X., Hu, N., Zeng, F., et al., 2015b. Mussel-inspired surface modification of magnetic@graphite nanosheets composite for efficient *Candida rugosa* lipase immobilization. J. Ind. Microbiol. Biotechnol. 42, 723–734.

Hou, C., Zhu, H., Li, Y.F., Li, Y.J., Wang, X.Y., Zhu, W.W., et al., 2015c. Facile synthesis of oxidic PEG-modified magnetic polydopamine nanospheres for *Candida rugosa* lipase immobilization. Appl. Microbiol. Biotechnol. 99, 1249–1259.

Hu, X., 2012. Synergistic toxic effects of nonylphenol and nonylphenol ethoxylate on *Moina macrocopa*. Jinan University (in Chinese).

Jousset, A., 2012. Ecological and evolutive implications of bacterial defences against predators. Environ. Microbiol. 14, 1830–1843.

Karci, A., 2014. Degradation of chlorophenols and alkylphenol ethoxylates, two representative textile chemicals, in water by advanced oxidation processes: The state of the art on transformation products and toxicity. Chemosphere 99, 1–18.

Lee, J., Isobe, T., Senna, M., 1996. Preparation of ultrafine Fe_3O_4 particles by precipitation in the presence of PVA at high pH. J. Colloid Interface Sci. 177, 490–494.

Li, Y.-G., Gao, H.-S., Li, W.-L., Xing, J.-M., Liu, H.-Z., 2009. situ magnetic separation and immobilization of dibenzothiophene-desulfurizing bacteria. Bioresour. Technol. 100, 5092–5096.

Li, Y., Du, X., Wu, C., Liu, X., Wang, X., An, Xu P., 2013. efficient magnetically modified microbial cell biocomposite for carbazole biodegradation. Nanoscale Res. Lett. 8, 522.

Lin, Y.-W., Yang, C.-C., Tuan, N.N., Huang, S.-L., 2016. Diversity of octylphenol polyethoxylate-degrading bacteria: With a special reference to *Brevibacterium* sp. TX4. Int. Biodeterior. Biodegrad. 115, 55–63.

Liu, Y., Ai, K., Polydopamine, Lu L., 2014. its derivative materials: synthesis and promising applications in energy, environmental, and biomedical fields. Chem. Rev. 114, 5057–5115.

Lu, H., 2013. Bio-adhesive magnetic nanoparticles preparation and applied for immobilization of *Gluconobacter oxydans*. J. East China Univ. Sci. Technol. (in Chinese).

Lu, A.-H., Salabas, E.L., Schüth, F., 2007a. Magnetic nanoparticles: synthesis, protection, functionalization, and application. Ange Chem Int Edit 46, 1222–1244.

Lu, J., Jin, Q., He, Y., Wu, J., 2007b. Biodegradation of nonylphenol polyethoxylates under Fe(III)-reducing conditions. Chemosphere 69, 1047–1054.

Lu, H., Ni, K., Wang, C., Black, K.C.L., Wei, D., Ren, Y., et al., 2012. A novel technique for in situ aggregation of *Gluconobacter oxydans* using bio-adhesive magnetic nanoparticles. Biotechnol. Bioeng. 109, 2970–2977.

Martín, M., Salazar, P., Villalonga, R., Campuzano, S., Pingarrón, J.M., González-Mora, J.L., 2014. Preparation of core–shell Fe_3O_4@poly(dopamine) magnetic nanoparticles for biosensor construction. J. Mater. Chem. B 2, 739–746.

Mrozik, A., Piotrowska-Seget, Z., 2010. Bioaugmentation as a strategy for cleaning up of soils contaminated with aromatic compounds. Microbiol. Res. 165, 363–375.

Mundra, R.V., Wu, X., Sauer, J., Dordick, J.S., Kane, R.S., 2014. Nanotubes in biological applications. Curr. Opin. Biotechnol. 28, 25–32.

Naylor, C.G., Mieure, J.P., Adams, W.J., Weeks, J.A., Castaldi, F.J., Ogle, L.D., et al., 1992. Alkylphenol ethoxylates in the environment. J. Am. Oil Chem. Soc. 69, 695–703.

Pan, Y., Du, X., Zhao, F., Xu, B., 2012. Magnetic nanoparticles for the manipulation of proteins and cells. Chem. Soc. Rev. 41, 2912–2942.

Staples, C., Mihaich, E., Carbone, J., Woodburn, K., Klecka, G., 2004. A weight of evidence analysis of the chronic ecotoxicity of nonylphenol ethoxylates, nonylphenol ether carboxylates, and nonylphenol. Hum. Ecol. Risk. Assess. 10, 999–1017.

Sun, H.-W., H-W, Hu, Wang, L., Yang, Y., Huang, G.-L., 2014. The bioconcentration and degradation of nonylphenol and nonylphenol polyethoxylates by *Chlorella vulgaris*. Int. J. Mol. Sci. 15, 1255.

Sun, P., Hui, C., Azim Khan, R., Du, J., Zhang, Q., Zhao, Y.-H., 2015. Efficient removal of crystal violet using Fe_3O_4-coated biochar: the role of the Fe_3O_4 nanoparticles and modeling study their adsorption behavior. Sci Rep 5, 12638.

Toyooka, T., Kubota, T., Ibuki, Y., 2012. Nonylphenol polyethoxylates induce phosphorylation of histone H2AX. Mutat. Res. Genet. Toxicol. Environ. Mutagen. 741, 57–64.

Wang, J., Xiong, L., Zhang, H., Chen, J., 2011. Determination of alkylphenol and alkylphenolpolyethoxylates in brine by solid phase extraction and high performance liquid chromatography-mass spectrometry. Chin. J. Chromatogr. 1160–1164 (in Chinese).

Xu, C., Xu, K., Gu, H., Zheng, R., Liu, H., Zhang, X., et al., 2004. Dopamine as a robust anchor to immobilize functional molecules on the iron oxide shell of magnetic nanoparticles. J. Am. Chem. Soc. 126, 9938–9939.

Xu, P., Zeng, G.M., Huang, D.L., Feng, C.L., Hu, S., Zhao, M.H., et al., 2012. Use of iron oxide nanomaterials in wastewater treatment: a review. Sci. Total Environ. 424, 1–10.

Yang, D., Li, X., Meng, D., Wang, M., Yang, Y., 2017. Supramolecular solvents combined with layered double hydroxide-coated magnetic nanoparticles for extraction of bisphenols and 4-tert-octylphenol from fruit juices. Food Chem. 237, 870–876.

Zakaria, B.S., Nassar, H.N., Saed, D., El-Gendy, N.S., 2015. Enhancement of carbazole denitrogenation rate using magnetically decorated *Bacillus clausii* BS1. Petrol. Sci. Technol. 33, 802–811.

Zhang, W., Li, L., Wang, C., Liu, C., Fan, X., Tang, L., 2007. Determination of alkylphenol and alkylphenolpolyethoxylates in textile by LC-MS. J. Instrum. Anal. 44–47 (in Chinese).

Zhuang, H., Han, H., Xu, P., Hou, B., Jia, S., Wang, D., et al., 2015. Biodegradation of quinoline by *Streptomyces* sp. N01 immobilized on bamboo carbon supported Fe_3O_4 nanoparticles. Biochem. Eng. J. 99, 44–47.